Biochemical and Biophysical Research Communications 445 (2014) 244–249

Contents lists available at ScienceDirect

Biochemical and Biophysical Research Communications

journal homepage: www.elsevier.com/locate/ybbrc

Annexin A7 deficiency potentiates cardiac NFAT activity promoting hypertrophic signaling

Jakob Voelkl [a], Ioana Alesutan [a], Tatsiana Pakladok [a], Robert Viereck [a], Martina Feger [a], Sobuj Mia [a], Tanja Schönberger [b], Angelika A. Noegel [c], Meinrad Gawaz [b], Florian Lang [a,*]

[a] Department of Physiology, University of Tübingen, Tübingen, Germany
[b] Department of Cardiology and Cardiovascular Medicine, University of Tübingen, Tübingen, Germany
[c] Center for Biochemistry, Institute of Biochemistry I, University of Cologne, Köln, Germany

ARTICLE INFO

Article history:
Received 28 January 2014
Available online 6 February 2014

Keywords:
NFAT
Annexin A7
HL-1 cardiomyocytes
Pressure overload

ABSTRACT

Annexin A7 (Anxa7) is a cytoskeletal protein interacting with Ca^{2+} signaling which in turn is a crucial factor for cardiac remodeling following cardiac injury. The present study explored whether Anxa7 participates in the regulation of cardiac stress signaling. To this end, mice lacking functional Anxa7 (anxa7$^{-/-}$) and wild-type mice (anxa7$^{+/+}$) were investigated following pressure overload by transverse aortic constriction (TAC). In addition, HL-1 cardiomyocytes were silenced with Anxa7 siRNA and treated with isoproterenol. Transcript levels were determined by quantitative RT-PCR, transcriptional activity by luciferase reporter assay and protein abundance by Western blotting and confocal microscopy. As a result, TAC treatment increased the mRNA and protein levels of Anxa7 in wild-type mice. Moreover, TAC increased heart weight to body weight ratio and the cardiac mRNA levels of *αSka*, *Nppb*, *Col1a1*, *Col3a1* and *Rcan1*, effects more pronounced in anxa7$^{-/-}$ mice than in anxa7$^{+/+}$ mice. Silencing of Anxa7 in HL-1 cardiomyocytes significantly increased nuclear localization of Nfatc1. Furthermore, Anxa7 silencing increased NFAT-dependent transcriptional activity as well as *αSka*, *Nppb*, and *Rcan1* mRNA levels both, under control conditions and following β-adrenergic stimulation by isoproterenol. These observations point to an important role of annexin A7 in the regulation of cardiac NFAT activity and hypertrophic response following cardiac stress conditions.

1. Introduction

Annexins, Ca^{2+}- and phospholipid-binding intracellular proteins [1–5], contribute to the regulation of diverse functions, such as inhibition of phospholipase A_2 [6,7], aggregation of chromaffin granules [8], crosslinking of proteins within the cell cortex [9], regulation of ion channels [10] as well as endo- and exocytosis [11,12]. Annexin A7 (or Anxa7, annexin VII, synexin) binds to secretory vesicles and participates in the regulation of secretion [13–15]. Anxa7 further participates in cellular Ca^{2+} signaling [16–18]. Anxa7 has been implicated in spherocytosis [19], inflammatory myopathies [20], cardiac remodeling [21], as well as regulation of cell survival and tumor growth [22–25].

The initially generated Anxa7 knockout mice were not viable but lethal on embryonic day 10 [26]. A second attempt yielded viable Anxa7 knockout mice [27], which suffer from impaired platelet function [28], enhanced glial cell proliferation [16] and enhanced suicidal erythrocyte death [29]. In Anxa7-deficient mice cardiomyocyte shortening-frequency relationship and cardiac excitation are altered [27,30].

In view of the role of Anxa7 in the regulation of Ca^{2+}-dependent processes [1], Anxa7 may be involved in the cardiac stress response following pressure overload, which has previously been shown to be modified by cytosolic Ca^{2+} activity. Hypertension or heart muscle injury may result in pathological cardiac hypertrophy, a key event in heart failure [31]. The present study thus explored the role of annexin A7 in cardiac hypertrophic signaling.

Abbreviations: Anxa7, annexin A7, annexin VII, synexin; *αSka*, α-skeletal actin; a.u., arbitrary units; *Col1a1*, collagen type I alpha1; *Col3a1*, collagen type III alpha1; ISO, isoproterenol; Gapdh, glyceraldehyde 3-phosphate dehydrogenase; NFAT, nuclear factor of activated T-cells; Nfatc1, nuclear factor of activated T-cells, cytoplasmic, calcineurin-dependent 1; *Nppb*, natriuretic peptide type B; TAC, transverse aortic constriction; *Rcan1*, regulator of calcineurin 1.

* Corresponding author. Address: Department of Physiology, University of Tübingen, Gmelinstr. 5, D-72076 Tübingen, Germany. Fax: +49 7071 295618.
E-mail address: florian.lang@uni-tuebingen.de (F. Lang).

http://dx.doi.org/10.1016/j.bbrc.2014.01.186
0006-291X/

2. Materials and methods

2.1. Animals

Experiments were performed in Anxa7 knockout mice (anxa7$^{-/-}$) [27]. 129SV mice were used as control (anxa7$^{+/+}$). All animal experiments were conducted according to the German law for the care and use of laboratory animals and were approved by the local authorities. The mice were fed standard rodent diet and had access to drinking water ad libitum. Cardiac pressure overload was induced by transverse aortic constriction (TAC) as described previously [32,33]. Briefly, male mice aged 10–13 weeks were anaesthetized by a mixture of midazolame (5 mg/kg b.w.), medetomidine (0.5 mg/kg b.w.) and fentanyl (0.05 mg/kg b.w.) and placed on a heating pad. After intubation and ventilation (Harvard minivent, Harvard apparatus), an intercostal space was opened by a small incision. The transverse aorta was exposed and constricted by the width of a 27-G canula using a 7-0 nylon suture. After closing of the access site, anesthesia was antagonized and animals were treated with buprenorphine (0.05 mg/kg b.w.) after procedure. High frequency 2D Echocardiography was performed 3 weeks after the TAC procedure (Vevo-2100 Imaging System, VisualSonics). Mice were sedated by 1.5% isoflurane via a breathing mask after induction with 5% isoflurane and placed supine on a temperature controlled heating platform with simultaneous ECG acquisition. The chest hair was removed and multiple long axis view images of the left ventricle were acquired, analyzed and results calculated by the internal software.

2.2. Cell culture of HL-1 cardiomyocytes

HL-1 cardiomyocytes (kindly provided by Dr. W.C. Claycomb, Department of Biochemistry and Molecular Biology, Louisiana State University) were maintained in Claycomb medium (Sigma Aldrich) supplemented with 10% FBS (Sigma Aldrich), 0.1 mM norepinephrine (Sigma Aldrich), 2 mM L-glutamine (Sigma Aldrich), 100 units/ml penicillin and 100 μg/ml streptomycin (Invitrogen). The medium was changed approximately every 24 h. HL-1 cardiomyocytes were seeded onto 0.02% gelatin/0.00125% fibronectin-coated dishes and cultured in normal growing medium. After 24 h, the cells were subsequently transfected with 10 nM Anxa7 siRNA (ID No. S62363, Ambion, Life Technologies) or with 10 nM negative control siRNA (ID No. 4390843, Ambion, Life Technologies) using siPORT amine transfection agent (Ambion, Life Technologies) according to the manufacturer's protocol. The cells were used 72 h after silencing. Silencing efficiency was verified by quantitative RT-PCR. The medium was changed to Claycomb medium supplemented with 2 mM L-glutamine, 100 units/ml penicillin and 100 μg/ml streptomycin 4 h prior to treatment with 10 μM isoproterenol bitartrate salt (Sigma Aldrich) for 24 h.

2.3. Quantitative RT-PCR

Total RNA was isolated from murine heart and from HL-1 cardiomyocytes using Trifast Reagent (Peqlab) according to the manufacturer's instructions. Reverse transcription of 2 μg RNA was performed using oligo(dT)$_{12-18}$ primers (Invitrogen) and SuperScript III Reverse Transcriptase (Invitrogen). cDNA samples were treated with RNase H (Invitrogen). Quantitative real-time PCR was performed with the iCycler iQ™ Real-Time PCR Detection System (Bio-Rad Laboratories) and iQ Sybr Green Supermix (Bio-Rad Laboratories) according to the manufacturer's instructions. The following primers were used (5′ → 3′ orientation): *Anxa7* fw: AAGCTCCCTACCCTAGCCAG; *Anxa7* rev: CCTTTCATTGCTTTGCGGAGA; *αSka* fw: CCCAAAGCTAACCGGGAGAAG; *αSka* rev: GACAGCACCGCCTGGATAG; *Col1a1* fw: ACCCGAGGTATGCTTGATCTG; *Col1a1* rev: CATTGCACGTCATCGCACAC; *Col3a1* fw: CCATTTGGAGAATGTTGTGCAAT; *Col3a1* rev: GGACATGATTCACAGATTCCAGG; *Gapdh* fw: AGGTCGGTGTGAACGGATTTG; *Gapdh* rev: TGTAGACCATGTAGTTGAGGTCA; *Rcan1* fw: AGCTCCCTGATTGCCTGTGT; *Rcan1* rev: TTTGGCCCTGGTCTCACTTT. The specificity of the PCR products was confirmed by analysis of the melting curves and in addition by agarose gel electrophoresis.

To determine *Bnp* (*Nppb*) transcript levels, quantitative real-time PCR was performed using Universal TaqMan Master Mix (Applied Biosystems) as recommended by the manufacturer. TaqMan primers and probes for *Nppb* and *Gapdh* were purchased from Applied Biosystems (Applied Biosystems). All PCRs were performed in duplicate and relative mRNA fold changes were calculated by the $2^{-\Delta\Delta Ct}$ method using *Gapdh* as internal reference.

2.4. Immunocytochemistry and confocal microscopy

For immunocytochemistry, HL-1 cardiomyocytes cultured onto 0.02% gelatin/0.00125% fibronectin-coated two-well chamber slides (BD Biostatus) were washed with PBS, fixed with 4% paraformaldehyde/PBS for 15 min at RT and permeabilized with PBS/ 0.1% Triton-X for 10 min at RT. After blocking with 5% normal goat serum in PBS/0.1% Triton-X for 1 h at RT, the slides were incubated overnight at 4 °C with rabbit polyclonal anti-Nfatc1 antibody (diluted 1:50, Santa Cruz Biotechnology). Binding of primary antibody was visualized using goat anti-rabbit Alexa Fluor488-conjugated antibody (diluted 1:1000, Invitrogen) incubated for 1 h at RT. Nuclei were stained using DRAQ-5 dye (diluted 1:1000, Biostatus) and actin using Rhodamine Phalloidin (diluted 1:100, Invitrogen). The slides were mounted with Prolong Gold antifade reagent (Invitrogen). Images were collected with a confocal laser-scanning microscope (LSM 510, Carl Zeiss MicroImaging GmbH) using a water immersion A-Plan ×63/1.2W. Confocal images are representative for 4 independent experiments. Negative controls were carried out simultaneously by omitting incubation with primary antibody.

2.5. Extraction of nuclear and cytoplasmic proteins

HL-1 cardiomyocytes cultured onto 0.02% gelatin/0.00125% fibronectin-coated culture dishes were washed with PBS, scraped off the dishes in ice-cold PBS, and centrifuged at 2000 rpm for 5 min. The preparation of cytoplasmic and nuclear extracts was performed using the NE-PER nuclear and cytoplasmic extraction reagents (Thermo Fisher Scientific) according to the manufacturer's instructions. Protein concentration was determined by Bradford assay (Biorad Laboratories) and 30 μg of proteins were boiled in Roti-Load1 Buffer (Carl Roth) at 100 °C for 10 min. Nfatc1 nuclear translocation was further determined by Western blot analysis.

2.6. Western blot analysis

Murine heart tissues were lysed with ice-cold lysis buffer (Thermo Fisher Scientific) supplemented with complete protease and phosphatase inhibitor cocktail (Thermo Fisher Scientific). After centrifugation at 10,000 rpm for 5 min, 30 μg of proteins were boiled in Roti-Load1 Buffer (Carl Roth) at 100 °C for 10 min. Proteins were separated on SDS–polyacrylamide gels and transferred to PVDF membranes. The membranes were incubated overnight at 4 °C with primary goat anti-Anxa7 antibody (diluted 1:1000, R&D Systems), rabbit monoclonal anti-Nfat2 antibody (diluted 1:1000, Cell Signaling), rabbit anti-Hdac2 antibody (diluted 1:1000, Cell Signaling), rabbit anti-α-tubulin antibody (diluted 1:1000, Cell Signaling) or rabbit anti-GAPDH antibody (diluted

1:1000, Cell Signaling) and then with secondary anti-goat HRP-conjugated antibody (diluted 1:2000, Santa Cruz Biotechnology) or secondary anti-rabbit HRP-conjugated antibody (diluted 1:1000, Cell Signaling) for 1 h at RT. For loading controls, the membranes were stripped in stripping buffer (Thermo Fisher Scientific) for 10 min at RT. Antibody binding was detected with the ECL detection reagent (Amersham) and bands were quantified using Quantity One Software (Bio-Rad). Results are shown as the ratio of Anxa7 to Gapdh protein normalized to the sham treated wild-type mice. For Nfac1 nuclear translocation, results are shown as the ratio of nuclear to cytoplasmic Nfatc1 protein normalized to Hdac2 or α-tubulin for the nuclear fraction or the cytoplasmic fraction, respectively.

2.7. Luciferase assay

HL-1 cardiomyocytes were co-transfected for 48 h with 1 μg DNA mixture of Nfat-responsive luciferase construct and a constitutively-expressing *Renilla* construct (40:1 ratio, Qiagen) using X-tremeGENE HP DNA transfection reagent (Roche) according to the manufacturer's protocol. *Renilla*-luciferase served as an internal control for the transfection efficiency. Cells were washed with ice-cold PBS, lysed with Passive Lysis Buffer (Promega), kept on ice for 15 min, centrifuged at 10,000 rpm at 4 °C and the supernatant stored at −80 °C. Samples were added in duplicate in a luminometry plate (20 μl/well) and read using the Dual-Luciferase Reporter Assay (Promega) in a luminometer (Walter Wallac 2 plate reader, Perkin Elmer). Relative light units (RLU) were obtained for both Nfat firefly-luciferase and *Renilla*-luciferase and all results are expressed as the ratio of Nfat firefly-luciferase to *Renilla*-luciferase normalized to the HL-1 cardiomyocytes silenced with negative control siRNA.

2.8. Statistics

Data are provided as means ± SEM, n represents the number of independent experiments. All data were tested for significance using t-test or Mann–Whitney test according to Shapiro–Wilk test and only results with $p < 0.05$ were considered statistically significant.

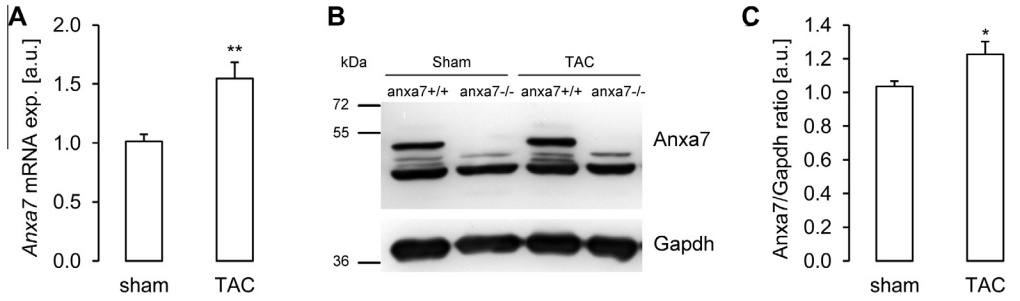

Fig. 1. Cardiac annexin A7 expression in wild-type mice following TAC. Arithmetic means ± SEM ((A), $n = 9$–10 mice/group; arbitrary units, a.u.) of *Anxa7* relative mRNA expression in cardiac tissue from wild-type mice (anxa7$^{+/+}$) following sham (sham, left bar) or transverse aortic constriction (TAC, right bar) procedure. Representative original Western blots (B) showing Anxa7 and Gapdh protein abundance in cardiac tissue from anxa7$^{+/+}$ mice and Anxa7 knockout mice (anxa7$^{-/-}$) following sham (sham) or transverse aortic constriction (TAC) procedure. Arithmetic means ± SEM ((C), $n = 10$ mice/group; a.u.) of normalized Anxa7 to Gapdh protein ratio in cardiac tissue from anxa7$^{+/+}$ mice following sham (sham, left bar) or transverse aortic constriction (TAC, right bar) procedure. *($p < 0.05$), **($p < 0.01$) statistically significant vs. sham treated anxa7$^{+/+}$ mice.

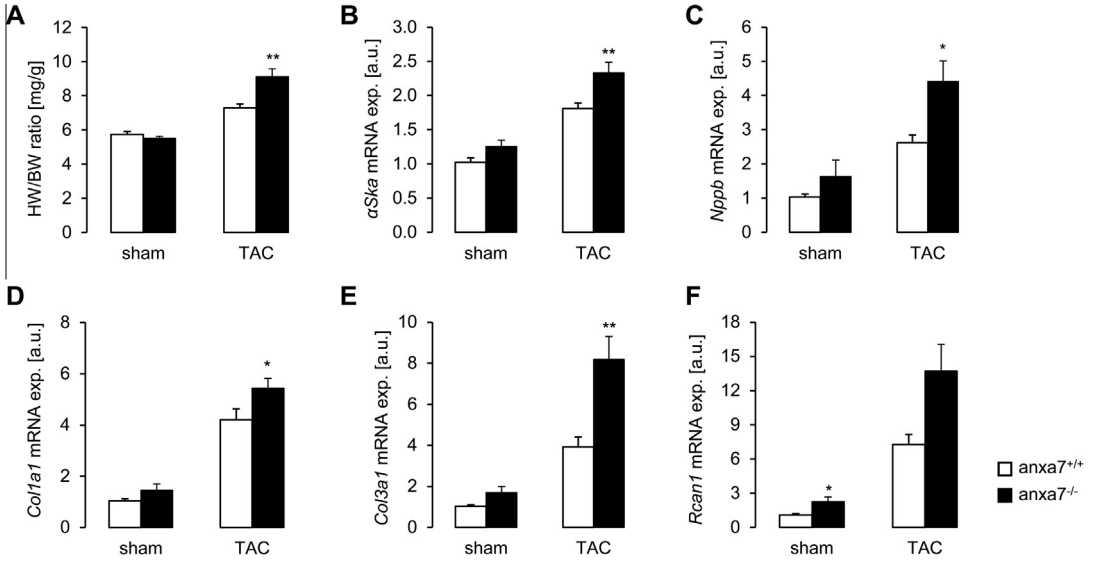

Fig. 2. Hypertrophic changes in cardiac tissue from anxa7$^{-/-}$ mice following TAC. Arithmetic means ± SEM ($n = 9$–13 mice/group) of heart weight to body weight ratio ((A); mg/g), and *αSka* ((B); arbitrary units, a.u), *Nppb* ((C); a.u.), *Col1a1* ((D); a.u.), *Col3a1* ((E); a.u.) and *Rcan1* ((F); a.u.) relative mRNA expression in cardiac tissue from wild-type mice (anxa7$^{+/+}$, white bars) and Anxa7 knockout mice (anxa7$^{-/-}$, black bars) following sham (sham, left columns) or transverse aortic constriction (TAC, right columns) procedure. *($p < 0.05$), **($p < 0.01$) statistically significant vs. respective anxa7$^{+/+}$ mice.

3. Results

To explore the impact of Anxa7 on cardiac remodeling, experiments were performed in mice lacking functional Anxa7 (anxa7$^{-/-}$) and in corresponding wild-type mice (anxa7$^{+/+}$). In order to impose pressure overload, the mice were subjected to transverse aortic constriction (TAC) for 3 weeks. As apparent in cardiac tissue from anxa7$^{+/+}$ mice, TAC was followed by a significant increase of *Anxa7* mRNA expression (Fig. 1A), an effect paralleled by a similar increase of Anxa7 protein abundance (Fig. 1B and C). No Anxa7 expression was detected in cardiac tissue from anxa7$^{-/-}$ mice.

As illustrated in Fig. 2A, the heart weight to body weight ratio increased following TAC treatment. This increase was significantly more pronounced in anxa7$^{-/-}$ mice as compared to anxa7$^{+/+}$ mice. TAC treatment tended to decrease the cardiac fractional shortening stronger in anxa7$^{-/-}$ mice, a difference, however, not reaching statistical significance (anxa7$^{+/+}$ sham: 28.3 ± 0.8%; anxa7$^{-/-}$ sham: 27.0 ± 2.5%; anxa7$^{+/+}$ TAC: 24.1 ± 1.5%; anxa7$^{-/-}$ TAC: 21.3 ± 1.2%; n = 11–13). The increase of the heart weight to body weight ratio

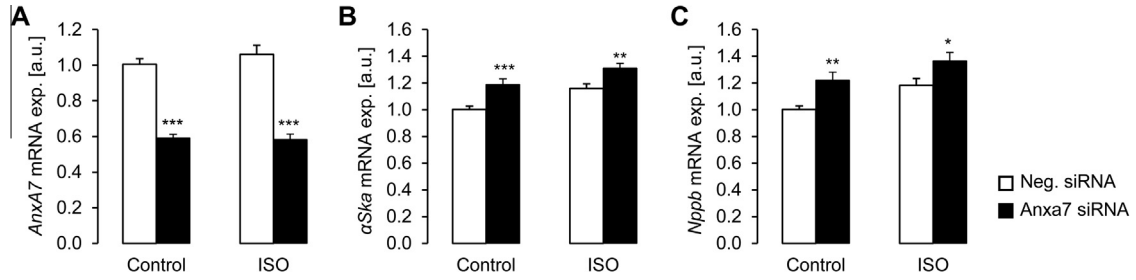

Fig. 3. Effect of annexin A7 silencing on HL-1 cardiomyocytes hypertrophy following β-adrenergic stimulation. Arithmetic means ± SEM (n = 12 independent experiments/group; arbitrary units, a.u.) of *Anxa7* (A), *αSka* (B) and *Nppb* (C) relative mRNA expression in HL-1 cardiomyocytes silenced for 72 h with negative control siRNA (Neg. siRNA, white bars) or Anxa7 siRNA (Anxa7 siRNA, black bars) without (Control, left columns) or with treatment for 24 h with 10 μM isoproterenol (ISO, right columns). *($p < 0.05$), **($p < 0.01$), ***($p < 0.001$) statistically significant vs respective Neg. siRNA silenced HL-1 cardiomyocytes.

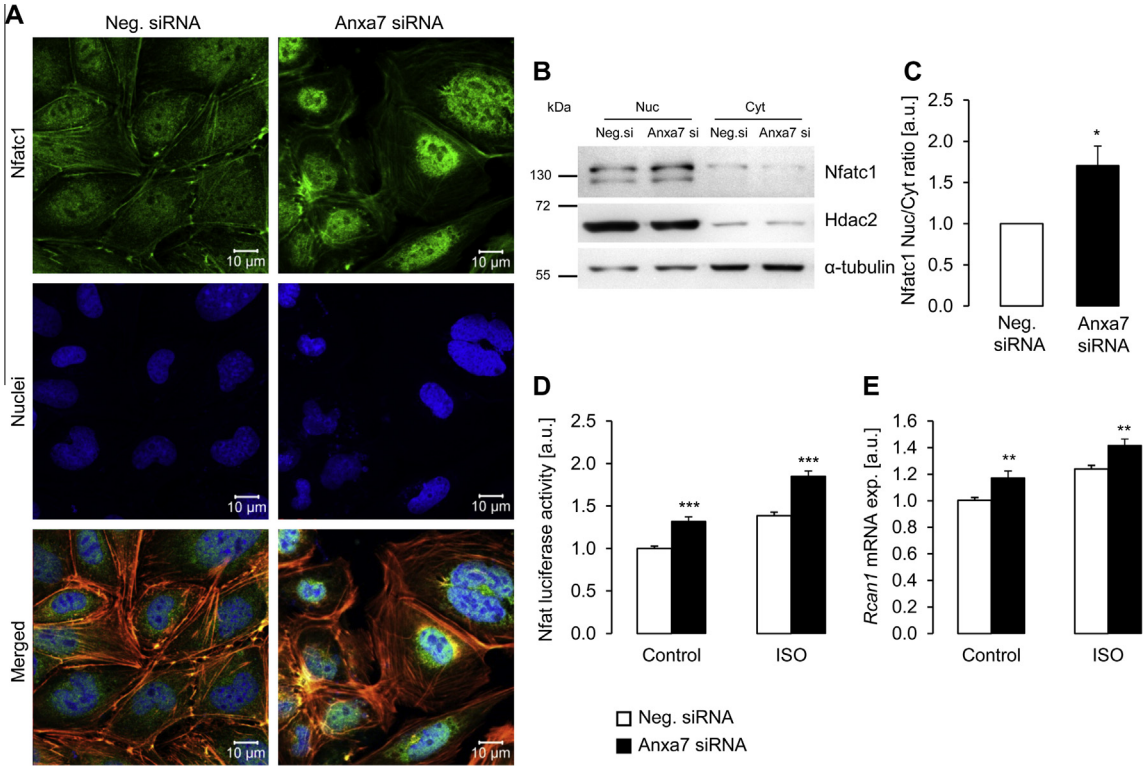

Fig. 4. Effect of annexin A7 silencing on NFAT activity in HL-1 cardiomyocytes. Confocal microscopy images (A) showing Nfatc1 protein expression and localization in HL-1 cardiomyocytes silenced for 72 h with negative control siRNA (Neg. siRNA) or Anxa7 siRNA (Anxa7 siRNA). Nfatc1 expression is represented by green labeling, nuclei are labeled in blue, and actin staining is labeled in red. Images are representative for four independent experiments. Representative original Western blots (B) and arithmetic means ± SEM ((C), n = 6 independent experiments/group; arbitrary units, a.u.) of normalized nuclear to cytoplasmic Nfatc1 protein ratio normalized to Hdac2 and α-tubulin protein in the nuclear fraction (Nuc) and cytoplasmic fraction (Cyt) respectively, of HL-1 cardiomyocytes silenced for 72 h with negative control siRNA (Neg. siRNA, white bar) or Anxa7 siRNA (Anxa7 siRNA, black bar). Arithmetic means ± SEM ((D), n = 6 independent experiments/group; a.u.) of NFAT-dependent transcriptional activity measured by luciferase reporter assay in HL-1 cardiomyocytes silenced for 72 h with negative control siRNA (Neg. siRNA, white bars) or Anxa7 siRNA (Anxa7 siRNA, black bars) without (Control, left columns) or with treatment for 24 h with 10 μM isoproterenol (ISO, right columns) and co-transfected for 48 h with NFAT-responsive Luciferase/*Renilla*-Luciferase constructs. Arithmetic means ± SEM ((E), n = 12 independent experiments/group; a.u.) of *Rcan1* relative mRNA expression in HL-1 cardiomyocytes silenced for 72 h with negative control siRNA (Neg. siRNA, white bars) or Anxa7 siRNA (Anxa7 siRNA, black bars) without (Control, left columns) or with treatment for 24 h with 10 μM isoproterenol (ISO, right columns). *($p < 0.05$), **($p < 0.01$), ***($p < 0.001$) statistically significant vs. respective Neg. siRNA silenced HL-1 cardiomyocytes. (For interpretation of the references to color in this figure legend, the reader is referred to the web version of this article.)

was paralleled by an increase of the cardiac α-skeletal actin (*αSka*) and natriuretic peptide type B (*Nppb*) mRNA expression (Fig. 2B and C). The effects were significantly higher in anxa7$^{-/-}$ mice than in anxa7$^{+/+}$ mice. Furthermore, TAC increased the mRNA levels of *Col1a1* and *Col3a1* to significantly higher levels in anxa7$^{-/-}$ mice as compared to anxa7$^{+/+}$ mice (Fig. 2D and E). The cardiac mRNA levels of calcineurin/NFAT target gene *Rcan1* (regulator of calcineurin 1) were higher in anxa7$^{-/-}$ mice than in anxa7$^{+/+}$ mice, an effect reaching significance in sham treated, but not in TAC treated animals (Fig. 2F).

Additional experiments were performed to investigate the role of Anxa7 in HL-1 cardiomyocytes hypertrophy. To this end, RNA interference was used to suppress endogenous *Anxa7* mRNA levels in HL-1 cardiomyocytes. Silencing efficiency was verified by quantitative RT-PCR (Fig. 3A). As illustrated in Fig. 3A, β-adrenergic stimulation by isoproterenol treatment had little effect on *Anxa7* mRNA levels. Nonetheless, silencing of Anxa7 significantly enhanced *αSka* mRNA expression, both in control conditions and following isoproterenol treatment (Fig. 3B). Similarly, the *Nppb* mRNA expression was significantly increased by silencing of Anxa7 in control and isoproterenol treated HL-1 cardiomyocytes (Fig. 3C).

Due to the effects of Anxa7 deficiency on cardiac hypertrophy markers, further experiments explored nuclear factor of activated T-cells (NFAT) as possible downstream mediator of Anxa7 deficiency. As illustrated in Fig. 4A, silencing of Anxa7 in HL-1 cardiomyocytes induced the nuclear localization of Nfatc1 as compared to negative control silenced HL-1 cardiomyocytes. This finding was parallelled by a significantly increased Nfatc1 protein abundance in the nuclear fraction of Anxa7 silenced HL-1 cardiomyocytes (Fig. 4B and C). A luciferase reporter assay was employed to further explore the transcriptional activation of NFAT. Anxa7 silencing significantly augmented NFAT-dependent transcriptional activity in HL-1 cardiomyocytes (Fig. 4D). Accordingly, Anxa7 silencing significantly increased transcript levels of *Rcan1*, a target gene of nuclear factor of activated T-cells (NFAT) (Fig. 4E). The effects were observed in both, control treated and isoproterenol treated HL-1 cardiomyocytes.

4. Discussion

The present observations reveal a role of annexin A7 in the regulation of cardiac NFAT activity and in the hypertrophic response following pressure overload. Anxa7 is apparently an inhibitor of cardiac Ca^{2+} signaling, thus blunting the activation of the Ca^{2+}-sensitive transcription factor NFAT following isoproterenol treatment and pressure overload. Even in control treated HL-1 cardiomyocytes, partial lack of Anxa7 is followed by enhanced NFAT activity and increased expression of NFAT target gene *Rcan1*. The effect of *in vivo* pressure overload by transverse aortic constriction (TAC) and the *in vitro* effect of isoproterenol on several genes reflecting the cardiac hypertrophic response were augmented in animals lacking functional Anxa7 and in HL-1 cardiomyocytes following silencing of Anxa7.

The transcription factor NFAT is crucially important in cardiac disease [34] and promotes myocardial hypertrophy [34]. Disruption of NFAT signaling reduces the cardiac hypertrophic response and pathological cardiac remodeling [35]. The activation of NFAT involves Ca^{2+}-dependent signaling [36]. As reported previously [30], Ca^{2+} homeostasis is dysregulated in Anxa7-deficient cardiomyocytes at high stimulation frequencies. Furthermore, Anxa7 interacts with the cardiac ryanodine receptor [17]. In view of the function of Anxa7 in other cell types as Ca^{2+}- and phospholipid-binding intracellular protein [1–5] and in view of the Anxa7 sensitivity of the Ca^{2+}-regulated transcription factor NFAT, the present observations are suggestive that Anxa7 is at least in part effective by blunting Ca^{2+}-dependent signaling. Nonetheless, the present observations do not rule out further, Ca^{2+}-independent Anxa7 sensitive mechanisms.

In conclusion, annexin A7 deficiency augments cardiac NFAT activity and promotes hypertrophic signaling in cardiomyocytes. The present observations thus reveal a novel player in the signaling of pathological cardiac remodeling.

Acknowledgments

The authors gratefully acknowledge Dr. William C. Claycomb for providing the HL-1 cardiomyocyte cell line and the meticulous preparation of the manuscript by Tanja Loch. This work was supported by the DFG (GRK 1302/1, KFO274).

References

[1] E. Camors, V. Monceau, D. Charlemagne, Annexins and Ca2+ handling in the heart, Cardiovasc. Res. 65 (2005) 793–802.
[2] V. Gerke, S.E. Moss, Annexins: from structure to function, Physiol. Rev. 82 (2002) 331–371.
[3] K. Monastyrskaya, E.B. Babiychuk, A. Hostettler, P. Wood, T. Grewal, A. Draeger, Plasma membrane-associated annexin A6 reduces Ca2+ entry by stabilizing the cortical actin cytoskeleton, J. Biol. Chem. 284 (2009) 17227–17242.
[4] K. Monastyrskaya, E.B. Babiychuk, A. Draeger, The annexins: spatial and temporal coordination of signaling events during cellular stress, Cell. Mol. Life Sci. 66 (2009) 2623–2642.
[5] P. Raynal, H.B. Pollard, Annexins: the problem of assessing the biological role for a gene family of multifunctional calcium- and phospholipid-binding proteins, Biochim. Biophys. Acta 1197 (1994) 63–93.
[6] F. Russo-Marie, Macrophages and the glucocorticoids, J. Neuroimmunol. 40 (1992) 281–286.
[7] H. Yoshizaki, S. Tanabe, K. Arai, A. Murakami, Y. Wada, M. Ohkuchi, Y. Hashimoto, M. Maki, Effects of calphobindin II (annexin VI) on procoagulant and anticoagulant activities of cultured endothelial cells, Chem. Pharm. Bull. (Tokyo) 40 (1992) 1860–1863.
[8] D.S. Drust, C.E. Creutz, Aggregation of chromaffin granules by calpactin at micromolar levels of calcium, Nature 331 (1988) 88–91.
[9] J.R. Glenney Jr., Calpactins: calcium-regulated membrane-skeletal proteins, Biochem. Soc. Trans. 15 (1987) 798–800.
[10] R. Huber, J. Romisch, E.P. Paques, The crystal and molecular structure of human annexin V, an anticoagulant protein that binds to calcium and membranes, EMBO J. 9 (1990) 3867–3874.
[11] S.M. Ali, M.J. Geisow, R.D. Burgoyne, A role for calpactin in calcium-dependent exocytosis in adrenal chromaffin cells, Nature 340 (1989) 313–315.
[12] N. Emans, J.P. Gorvel, C. Walter, V. Gerke, R. Kellner, G. Griffiths, J. Gruenberg, Annexin II is a major component of fusogenic endosomal vesicles, J. Cell Biol. 120 (1993) 1357–1369.
[13] H. Caohuy, M. Srivastava, H.B. Pollard, Membrane fusion protein synexin (annexin VII) as a Ca2+/GTP sensor in exocytotic secretion, Proc. Natl. Acad. Sci. USA 93 (1996) 10797–10802.
[14] C.S. Clemen, A. Hofmann, C. Zamparelli, A.A. Noegel, Expression and localisation of annexin VII (synexin) isoforms in differentiating myoblasts, J. Muscle Res. Cell Motil. 20 (1999) 669–679.
[15] G.A. Kuijpers, G. Lee, H.B. Pollard, Immunolocalization of synexin (annexin VII) in adrenal chromaffin granules and chromaffin cells: evidence for a dynamic role in the secretory process, Cell Tissue Res. 269 (1992) 323–330.
[16] C.S. Clemen, C. Herr, N. Hovelmeyer, A.A. Noegel, The lack of annexin A7 affects functions of primary astrocytes, Exp. Cell Res. 291 (2003) 406–414.
[17] G. Colotti, C. Zamparelli, D. Verzili, M. Mella, C.M. Loughrey, G.L. Smith, E. Chiancone, The W105G and W99G sorcin mutants demonstrate the role of the D helix in the Ca(2+)-dependent interaction with annexin VII and the cardiac ryanodine receptor, Biochemistry 45 (2006) 12519–12529.
[18] D. Mears, C.L. Zimliki, I. Atwater, E. Rojas, M. Glassman, X. Leighton, H.B. Pollard, M. Srivastava, The Anx7(+/−) knockout mutation alters electrical and secretory responses to Ca(2+)-mobilizing agents in pancreatic beta-cells, Cell. Physiol. Biochem. 29 (2012) 697–704.
[19] M. Caterino, M. Ruoppolo, S. Orru, M. Savoia, S. Perrotta, L. Del Vecchio, F. Salvatore, G.W. Stewart, A. Iolascon, Characterization of red cell membrane proteins as a function of red cell density: annexin VII in different forms of hereditary spherocytosis, FEBS Lett. 580 (2006) 6527–6532.
[20] S. Probst-Cousin, C. Berghoff, B. Neundorfer, D. Heuss, Annexin expression in inflammatory myopathies, Muscle Nerve 30 (2004) 102–110.
[21] T. Urashima, M. Zhao, R. Wagner, G. Fajardo, S. Farahani, T. Quertermous, D. Bernstein, Molecular and physiological characterization of RV remodeling in a murine model of pulmonary stenosis, Am. J. Physiol. Heart Circ. Physiol. 295 (2008) H1351–H1368.
[22] P.I. Hsu, M.S. Huang, H.C. Chen, P.N. Hsu, T.C. Lai, J.L. Wang, G.H. Lo, K.H. Lai, C.J. Tseng, M. Hsiao, The significance of ANXA7 expression and its correlation with poor cellular differentiation and enhanced metastatic potential of gastric cancer, J. Surg. Oncol. 97 (2008) 609–614.

[23] M. Srivastava, Y. Torosyan, M. Raffeld, O. Eidelman, H.B. Pollard, L. Bubendorf, ANXA7 expression represents hormone-relevant tumor suppression in different cancers, Int. J. Cancer 121 (2007) 2628–2636.
[24] Y. Torosyan, O. Simakova, S. Naga, K. Mezhevaya, X. Leighton, J. Diaz, W. Huang, H. Pollard, M. Srivastava, Annexin-A7 protects normal prostate cells and induces distinct patterns of RB-associated cytotoxicity in androgen-sensitive and -resistant prostate cancer cells, Int. J. Cancer 125 (2009) 2528–2539.
[25] Y. Torosyan, A. Dobi, M. Glasman, K. Mezhevaya, S. Naga, W. Huang, C. Paweletz, X. Leighton, H.B. Pollard, M. Srivastava, Role of multi-hnRNP nuclear complex in regulation of tumor suppressor ANXA7 in prostate cancer cells, Oncogene 29 (2010) 2457–2466.
[26] M. Srivastava, I. Atwater, M. Glasman, X. Leighton, G. Goping, H. Caohuy, G. Miller, J. Pichel, H. Westphal, D. Mears, E. Rojas, H.B. Pollard, Defects in inositol 1,4,5-trisphosphate receptor expression, Ca(2+) signaling, and insulin secretion in the anx7(+/−) knockout mouse, Proc. Natl. Acad. Sci. USA 96 (1999) 13783–13788.
[27] C. Herr, N. Smyth, S. Ullrich, F. Yun, P. Sasse, J. Hescheler, B. Fleischmann, K. Lasek, K. Brixius, R.H. Schwinger, R. Fassler, R. Schroder, A.A. Noegel, Loss of annexin A7 leads to alterations in frequency-induced shortening of isolated murine cardiomyocytes, Mol. Cell. Biol. 21 (2001) 4119–4128.
[28] C. Herr, C.S. Clemen, G. Lehnert, R. Kutschkow, S.M. Picker, B.S. Gathof, C. Zamparelli, M. Schleicher, A.A. Noegel, Function, expression and localization of annexin A7 in platelets and red blood cells: insights derived from an annexin A7 mutant mouse, BMC Biochem. 4 (2003) 8.
[29] E. Lang, P.A. Lang, E. Shumilina, S.M. Qadri, Y. Kucherenko, D.S. Kempe, M. Föller, A. Capasso, T. Wieder, E. Gulbins, C.S. Clemen, C. Herr, A.A. Noegel, S.M. Huber, F. Lang, Enhanced eryptosis of erythrocytes from gene-targeted mice lacking annexin A7, Pflügers Arch. 460 (2010) 667–676.
[30] J.W. Schrickel, K. Brixius, C. Herr, C.S. Clemen, P. Sasse, K. Reetz, C. Grohe, R. Meyer, K. Tiemann, R. Schroder, W. Bloch, G. Nickenig, B.K. Fleischmann, A.A. Noegel, R.H. Schwinger, T. Lewalter, Enhanced heterogeneity of myocardial conduction and severe cardiac electrical instability in annexin A7-deficient mice, Cardiovasc. Res. 76 (2007) 257–268.
[31] B.C. Bernardo, K.L. Weeks, L. Pretorius, J.R. McMullen, Molecular distinction between physiological and pathological cardiac hypertrophy: experimental findings and therapeutic strategies, Pharmacol. Ther. 128 (2010) 191–227.
[32] H.A. Rockman, R.S. Ross, A.N. Harris, K.U. Knowlton, M.E. Steinhelper, L.J. Field, J. Ross Jr., K.R. Chien, Segregation of atrial-specific and inducible expression of an atrial natriuretic factor transgene in an in vivo murine model of cardiac hypertrophy, Proc. Natl. Acad. Sci. USA 88 (1991) 8277–8281.
[33] J. Voelkl, Y. Lin, I. Alesutan, M.S. Ahmed, V. Pasham, S. Mia, S. Gu, M. Feger, A. Saxena, B. Metzler, D. Kuhl, B.J. Pichler, F. Lang, Sgk1 sensitivity of Na(+)/H(+) exchanger activity and cardiac remodeling following pressure overload, Basic Res. Cardiol. 107 (2012) 236.
[34] B.J. Wilkins, Y.S. Dai, O.F. Bueno, S.A. Parsons, J. Xu, D.M. Plank, F. Jones, T.R. Kimball, J.D. Molkentin, Calcineurin/NFAT coupling participates in pathological, but not physiological, cardiac hypertrophy, Circ. Res. 94 (2004) 110–118.
[35] Q. Liu, Y. Chen, M. Auger-Messier, J.D. Molkentin, Interaction between NFkappaB and NFAT coordinates cardiac hypertrophy and pathological remodeling, Circ. Res. 110 (2012) 1077–1086.
[36] B.J. Wilkins, J.D. Molkentin, Calcium–calcineurin signaling in the regulation of cardiac hypertrophy, Biochem. Biophys. Res. Commun. 322 (2004) 1178–1191.